Applied Catalysis B: Environmental 178 (2015) 117–123

Contents lists available at ScienceDirect

Applied Catalysis B: Environmental

journal homepage: www.elsevier.com/locate/apcatb

Titanium dioxide sol–gel-coated expanded clay granules for use in photocatalytic fluidized-bed reactor

Natalja Pronina[a,*], Deniss Klauson[a], Anna Moiseev[b], Joachim Deubener[b], Marina Krichevskaya[a]

[a] Department of Chemical Engineering, Tallinn University of Technology, Ehitajate tee 5, 19086 Tallinn, Estonia
[b] Institute of Non-Metallic Materials, TU Clausthal, Zehntnerstrasse 2a, 38678 Clausthal-Zellerfeld, Germany

ARTICLE INFO

Article history:
Received 22 June 2014
Received in revised form 9 September 2014
Accepted 5 October 2014
Available online 21 October 2014

Keywords:
Doxycycline elimination
Photocatalytic coating
Fluidized bed
Expanded clay granules.

ABSTRACT

An experimental research into the titania coatings on granulated expanded clay to be used in fluidized-bed photocatalytic reactor was undertaken. The preparation procedures were performed via sol–gel method using dip coating techniques. Two sol–gel compositions based on tetrabutyl orthotitanate and titanium tetraisopropoxide as well as two commercial TiO_2 sols were examined. The impacts of titania precursor concentration, modification of sol–gel by industrially available TiO_2 nanoparticles, the substrate withdrawal speed and thermal treatment conditions on the coatings' properties were studied. The photocatalytic activity of expanded clay-supported titania was evaluated by the degradation of an emerging micropollutant, tetracycline family antibiotic doxycycline. Mechanically stable and active coatings with properties dependent on sol–gel processing parameters were obtained. The application of porous titania sol–gel-coated expanded clays could combine pollutants' adsorption and their photocatalytic degradation. The compromise between coatings' improved photocatalytic performance, on the one hand, and their adhesion and attrition properties, significant for fluidized-bed operation, on the other hand, lead to the determination of appropriate processing parameters.

1. Introduction

The presence of pharmaceuticals in the environment has received a lot of attention in the last decades due to their negative health and environmental effects even at low concentrations [1,2]. Particularly, the occurrence of antibiotics in hospital, residential, dairy and livestock effluents and municipal wastewater with these pollutants passing through the conventional wastewater treatment intact causes their emissions and accumulation in the hydrological environment [3,4]. The pharmaceuticals are regularly monitored at low concentrations (mostly detected at ng L^{-1} levels) all over the world and the introduction of their obligatory monitoring is currently under discussion [5,6].

The public concern on pharmaceuticals in the environment demands the completion of wastewater treatment plants by the technologies for their removal. One of the options for the destructive elimination of such biologically persistent pollutants in wastewater is the use of advanced oxidation processes based on the action of reactive oxygen species. Amongst these technologies, the reactive species formed by photoexcitation of titanium dioxide allow degrading antibiotics [7–9]. Photocatalytic oxidation of tetracycline family antibiotic doxycycline was studied by our group [9] using P25 and sol–gel-synthesized titania slurries with oxidation by-products determined by liquid chromatography combined with mass spectrometry allowing to suggest the reaction pathway. Process favoring pH values, adsorption and photocatalytic reaction rate constants were obtained. Despite obvious ability of photocatalysis to degrade recalcitrant water pollutants, there is a need for the development of reactors and techniques for the catalyst attachment to the bed material.

Different materials were applied as titania photocatalyst support including glass, silica, ceramics, zeolites, stainless steel, activated carbon as well as granular materials like quartz sand, polymers, etc. [10–23]. Fixed-bed reactors have an intrinsic advantage of not requiring the catalyst separation operation, whereas fluidized-bed reactors are considered to reduce mass transfer limitations if compared to fixed bed. These, however, require the lightweight granular material with developed surface area.

* Corresponding author. Tel.: +372 6202851; fax: +372 6202856.
E-mail addresses: natalja.pronina@ttu.ee (N. Pronina), deniss.klauson@ttu.ee (D. Klauson), anna.moiseev@tu-clausthal.de (A. Moiseev), joachim.deubener@tu-clausthal.de (J. Deubener), marina.kritsevskaja@ttu.ee (M. Krichevskaya).

http://dx.doi.org/10.1016/j.apcatb.2014.10.006
0926-3373/

The present study is focused on the preparation of titania coatings on expanded clay granules to be applied in fluidized-bed reactor for the photocatalytic degradation of doxycycline antibiotic.

The lightweight ceramic expanded clays are rarely used as support material, and its utilization for the titania photocatalyst attachment was studied by our group as reported in [9] and by Zendehzaban et al. [24]. In the last study, the adsorption of titania from its propanolic suspensions on expanded clay granules with those floating on the surface of treated ammonia solutions was investigated. However, our previous study showed that the immobilization of titania on expanded clay from its aqueous or propanolic suspensions had not provided the appropriate adhesion of the catalyst onto the support resulting in a catalyst washout during fluidized bed operation. The application of tetraethyl orthosilicate (TEOS)-based sol–gel as a fixator for industrial photocatalyst nanoparticles showed relatively low activity of the coatings if compared to those obtained later with the titania sol–gel.

Due to the attrition and thus the high level of mechanical stress placed on the coated material, the emphasis on the study of adhesion and abrasion resistance properties of the titania coatings should be firstly done. Secondly, the photocatalytic activity of the bed material should be optimized within the acceptable mechanical properties of the coatings.

In this study, the authors tried to overcome the above-discussed issues by the consecutive investigation of several titania precursors based sol–gel compositions to produce coatings on expanded clay with improved photocatalytic and mechanical properties.

2. Experimental

2.1. Preparation of coatings

The titania coatings were prepared on preliminary sieved 2–3 mm fraction of lightweight expanded clay aggregates (Saint-Gobain Leca). Four sol–gel coating solutions based on two different titania precursors, such as tetrabutyl orthotitanate (TBOT, Fluka), titanium tetraisopropoxide (TTIP, Alfa Aesar) and two industrial sols Hombikat XXS 100 (Sachtleben Chemie) [25] and S5-300A (Cristal Chemical Company) [26], were examined.

The mixture of Hombikat XXS 100 and ethanol in a mass ratio of 1:4.1, respectively, was used in the Hombikat XXS 100 based coating procedure (procedure 1); S5-300A sol was applied as coating solution either diluted with ethanol (1:1.4, wt%) or as received (procedure 2).

TBOT-based solution (procedure 3) included addition of ethyl acetoacetate (Fluka) in amount of 1.63–5 g of 2-propanol under continuous stirring. TBOT in appropriate amount of 4.25 and 9.12 g of 2-propanol with preliminary dispersed P25 (Evonik) (9 wt% in 2-propanol) were added slowly to the sol–gel solution.

In TTIP-based coating solution (procedure 4), diethanolamine (DEA, Riedel-de-Haen) of 4.2 g was mixed with 5.6 g of 2-propanol. Then 2.84 g of TTIP and 0.72 g of H_2O were added dropwise under vigorous stirring. Subsequently to 24 h of stirring, 10 g of P25 propanolic suspension were added to the sol–gel solution and final sol was stirred overnight. The sol–gel-coated clay granules without P25 nanoparticles addition to the sol–gel solution were also prepared.

The coatings were prepared by means of dip coating technique. The clay granules were immersed in the sol–gel solution for 10 s and then withdrawn at 1 mm s^{-1} (dip coating machine, Vitando OÜ).

Sol–gel-coated clay granules were treated as follows: the pre-drying stage was performed at 120 °C for 1 or 2 h with temperature increasing rate of 30 °C min^{-1} (procedures 1–3 and 4, respectively). Afterwards, the coatings were dried at 200 °C for 2 h with temperature increasing rate of 30 °C min^{-1} (procedure 1) or calcined at 500 °C for 2 h with temperature increasing rate of 50 °C min^{-1} (procedures 2 and 4) or for 1 h with a rate of 8 °C min^{-1} (procedure 3).

The dipping and drying stages (procedures 3 and 4) were repeated also three times to vary the thickness of sol–gel coatings. Following the third drying step, the samples were heated for 2 h at 500 °C.

The coatings obtained by the procedure 4 were found to be the most stable and effective in doxycycline removal (see Section 3.2). Therefore, the influence of following parameters was studied to further improve the coatings properties: substrate withdrawal speed in the range of 0.5–2.0 mm s^{-1}, calcination temperature 400–600 °C and duration 1–3 h, P25 nanopowder and TTIP precursor concentration of 0–5.5 and 9.9–15.3 wt% in coating solution, respectively.

2.2. Experimental setup of photocatalytic oxidation

Two borosilicate glass tube units with an inner diameter of 30 mm and height of 370 mm with an aperture 146 m^2 m^{-3} were used as reaction vessels. Glass air diffusers were installed at the bottom of each reactor providing the clay granules' fluidization by pressurized air. To take into the account the effect of pollutants' adsorption onto the coated porous clay granules, one reactor was irradiated by the UV-A sources and another was operated in the dark (reference). The UV source consisted of two 15 W low-pressure mercury lamps (Philips Actinic BL) with a maximum emission at 365 nm and UV-B/UV-A ratio of less than 0.2%. Radiation loss was prevented by four flat reflectors positioned around the setup. The average UV-A irradiation intensity was ca. 9 W m^{-2} measured by fiber-optic spectrometer (USB2000 + UV-VIS-ES, Ocean Optics Inc.). The reaction temperature was maintained at 25 ± 2 °C.

Photocatalytic oxidation of 200 mL of doxycycline hyclate (AppliChem) solution with an initial doxycycline concentration of 25 mg L^{-1} was performed with 3.5 g of coated clay granules for 3 h.

The doxycycline concentration was analyzed by the high-performance liquid chromatography combined with diode array detector and mass spectrometer (HPLC-PDA-MS, Shimadzu LC-MS 2020). Phenomenex Gemini-NX 5u C18 110A 150 × 2.0 mm column, inner diameter 1.7 μm, was used with two eluents, 0.1% acetic acid aqueous solution (eluent A), and acetonitrile (eluent B), with total eluents flow of 0.3 mL min^{-1}; starting concentration of eluent B was 5%, increased to 48.5% by 23 min with linear gradient, held at that concentration for 2 min, and then decreased to 9.5% by 30 min, out of 30 min analysis. Mass spectra were acquired in full-scan mode, MS operated in positive ionization mode with interface voltage of 4.5 kV, and detector voltage of 1.1 kV. Diode array detector was set to scan samples at 190–800 nm. The instrument was operated and the results obtained with MS and PDA detectors were handled using Shimadzu LabSolutions software.

Scanning electron microscopy (SEM; Zeiss EVO 50 and EVO MA-15) was performed to visualize the catalyst coating. The structural stability and abrasion resistance of the coatings were characterized by the turbidity of the solutions measured during the fluidized-bed treatment process at 860 nm in Formazin Attenuation Units (FAU turbidity, Hach DR2800). The specific surface area of coated and bare expanded clay granules was measured by Areameter Ströhlein.

To express the results of doxycycline degradation and evaluate the activity of obtained sol–gel-coated clay granules, the photocatalytic oxidation efficiency E, mg W^{-1} h^{-1} [27], defined as the decrease in the amount of the pollutant in mg, divided by the product of UV-A radiation intensity, in W m^{-2}, the surface of the treated solution, in m^2, and irradiation time, in h, was used. The photocatalytically oxidized amount of doxycycline was calculated as the difference between doxycycline quantities removed in photocatalytic and reference experiments. The first number is taking

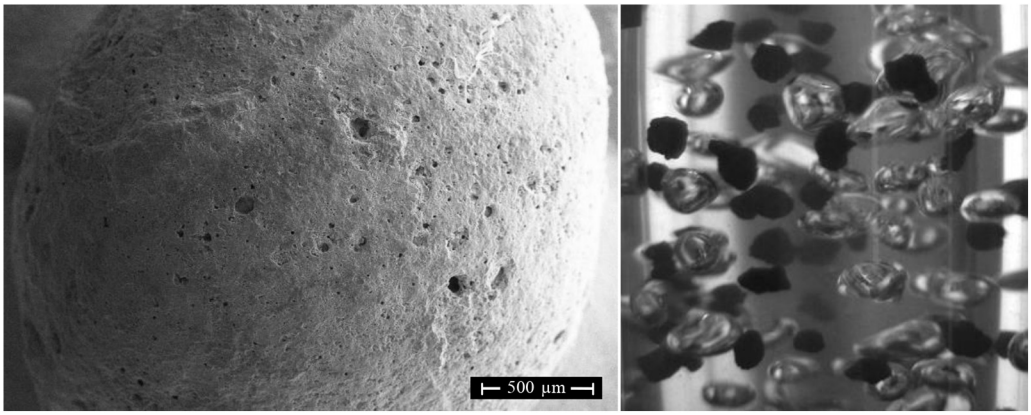

Fig. 1. SEM image of clay granule (left). Fluidized-bed operation of selected fraction of expanded clay granules (right).

into account the doxycycline removal by the net effect of oxidation and adsorption and the second one—removal in the course of dark adsorption. Thus, the effect of adsorption is subtracted from the *E*.

3. Results

The calculated external surface area of granules (Fig. 1, left) with average diameter of ca. 2.7 mm comprises approximately 0.004 $m^2 g^{-1}$, whereas the measured specific surface area of bare expanded clay granules of this particular fraction is ca. 0.8 $m^2 g^{-1}$. This porous lightweight granular material could be easily fluidized (Fig. 1, right).

Inorganic expanded clay granules could presumably serve as an adsorbent for the target pollutants and this should be taken into account for the evaluation of photocatalytic functionality of coated materials. For example, the overall doxycycline removal of over 3.4 mg (of initial 5 mg) was observed in 3 h, whereas considering the reference experimental runs (adsorption effects), the amount of doxycycline degraded in photocatalytic reaction reached 1.8 mg. To eliminate the doxycycline dark adsorption, all the reference experiments were carried out with expanded clay granules coated by the respective procedure.

The coatings prepared via procedures 1–4 were thoroughly studied firstly for their mechanical stability and secondly for the photocatalytic activity.

3.1. Industrial sol and TBOT-based sol–gel coatings

The materials prepared using ethanol-diluted Hombikat XXS and S5-300A solutions exhibited the low mechanical stability with high titania washout causing high turbidity levels of treated doxycycline solutions (up to 160 FAU). In the case of coatings obtained from TBOT precursor based sol–gel (procedure 3), sediments and the relatively high levels of turbidity (up to 60 FAU) were also observed presumably as a result of the incomplete hydrolysis and polycondensation reactions in sol and gel during the coating preparation procedure. The more intensive infiltration of low-viscose TBOT sol–gel solutions in the porous ceramic support, as possible explanation, could require the prolonged pre-drying step after dip coating and has led to the discarding of this sol–gel composition in the subsequent study.

Thus, the coatings with Hombikat XXS 100, S5-300A and TBOT used as titania sources (procedures 1–3) were not considered to be long-term effective mostly due to higher detachment levels of coatings' layers if compared with those prepared from different compositions of TTIP/DEA route described further. Although the photocatalytic efficiency of a number of materials prepared via 1–3 procedures approximated to the values of TTIP-based coatings efficiency, the higher turbidity and thus the shorter potential operating lifetime in fluidized-bed photocatalytic reactor narrowed down the choice of the most promising coating synthesis procedure to TTIP route. TTIP sol–gel-based dip coating resulted in materials of significantly higher abrasion resistance with the turbidity levels observed in the range of 0–40 FAU.

3.2. TTIP-based sol–gel coatings

The SEM micrographs of bare and TTIP-based sol–gel-coated expanded clay granules are shown in Fig. 2. The sol–gel coatings are smoothing the surface if compared to uncoated materials with no cracks observed if the particular (as described further) sol–gel solutions' composition and dip coating process parameters are in use.

Further, the adhesion and abrasion properties and photocatalytic activity of TTIP-based coatings were studied varying components' proportions in the sol–gel solutions and process parameters: 2-propanol content, amount of P25 nanoparticles to increase the photocatalyst weight, the substrate withdrawal speed as well as the temperature and duration of calcination step (Table 1).

The coatings with titania crystallized from TTIP showed explicitly measurable photocatalytic activity of up to 1.5 mg $W^{-1} h^{-1}$ with zero levels of turbidity in treated solutions.

The addition of P25 to the TTIP sol–gel as nanocrystalline photocatalyst source resulted in higher photocatalytic activities (up to 2.3 mg $W^{-1} h^{-1}$) along with different levels of nanoparticles washout causing the increase in solutions' turbidity in the range between 17 and 28 FAU (see Table 1; series of experiments I). The specific surface area of coated and bare expanded clay was measured to be very close: 1.0 and 0.8 $m^2 g^{-1}$, respectively, as well as the dark adsorption showed almost no difference in the respective amount of doxycycline adsorbed. The use of ultrasonication of P25 2-propanol suspension before its addition to the sol–gel solution lowered washout of nanoparticles (from 17 to 13 FAU) showing no changes in the coatings activity. The morphology of clay coated with P25 modified sol–gel composition is shown in Fig. 3. The primary particles of P25 titania could be distinguished on the micrograph with higher magnification, while the coating's surface is non-uniform: regions with P25 embedded in the sol–gel are alternating with smooth ones (Fig. 3, left).

The decrease in DEA to 2-propanol mass ratio (Table 1, Series II) lowered the activity of coated expanded clay (2.3–1.4 mg $W^{-1} h^{-1}$, Fig. 4). At the same time, the highest mechanical stability (lowest turbidity during fluidized-bed operation), within the series, was observed with the coated materials prepared from the sol with DEA to 2-propanol ratio of 0.29 (27 FAU). In a similar manner, the faster withdrawal speed (Table 1, Series III) had the positive effect on the coated clay's activity raising this up to 1.9 mg $W^{-1} h^{-1}$ (Fig. 4)

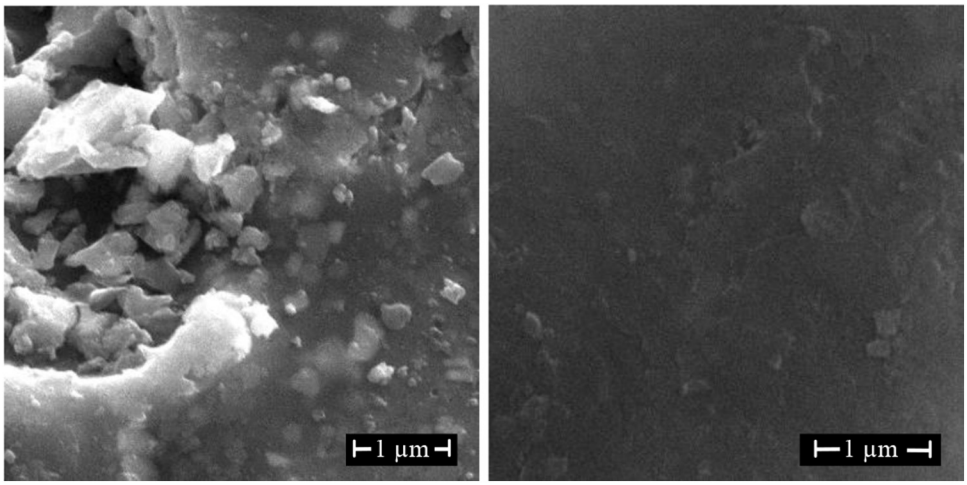

Fig. 2. SEM images of bare (left) and TTIP-based sol–gel-coated (right) expanded clay.

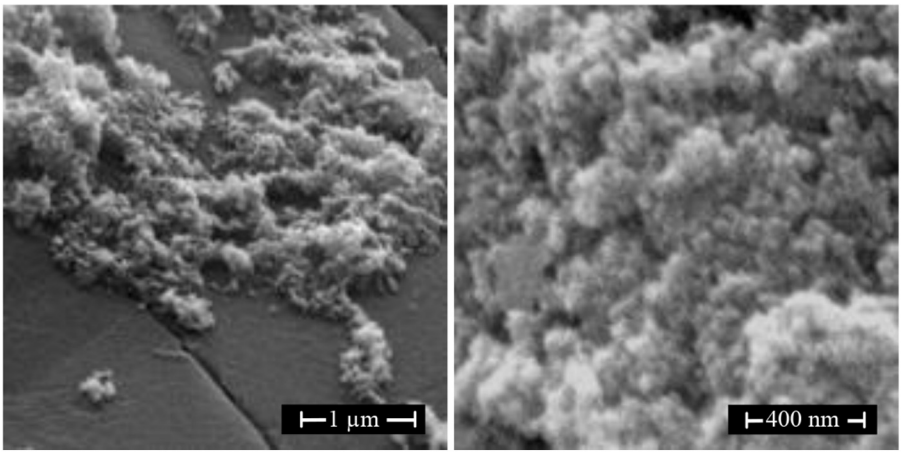

Fig. 3. SEM images of P25-modified sol–gel coatings at different magnifications.

with turbidity levels growing up to 29 FAU. The repetitive dip coating steps applied resulted in higher activity (1.7–2.1 mg W^{-1} h^{-1}), but also weakened the coatings' adhesion followed by the increase in turbidity of up to 40 FAU. However, the effect of intermediate calcination procedure could improve the mechanical stability of thicker TTIP based coatings (not studied here).

The variations in sol viscosity due to the changes in 2-propanol content, in the support withdrawal speed and in the number of

Table 1
Consolidated data on TTIP-based coatings (numbers in bold were considered to be the optimum).

Series of exp.	Sol–gel composition		Process parameters			Coatings performance	
	P25 (wt%)	2-Propanol (g)	Withdrawal speed (mm s^{-1})	Calcination temperature (°C)	Calcination time (h)	Photocat. eff. (mg W^{-1} h^{-1})	Turbidity (FAU)
I	0.0	14.7	1.0	500	2	1.5	0
	2.0					**1.6**	**17**
	3.9					1.7	27
	5.5					2.3	28
II	3.9	9.8	1.0	500	2	**2.3**	**32**
		14.7				1.7	27
		19.7				1.4	36
III	3.9	14.7	0.5	500	2	1.6	20
			1.0			**1.7**	**27**
			2.0			1.9	29
IV	3.9	14.7	1.0	400	2	1.4	29
				500		**1.7**	**27**
				600		1.7	27
V	3.9	14.7	1.0	500	1	**1.8**	**23**
					2	1.7	27
					3	1.9	31

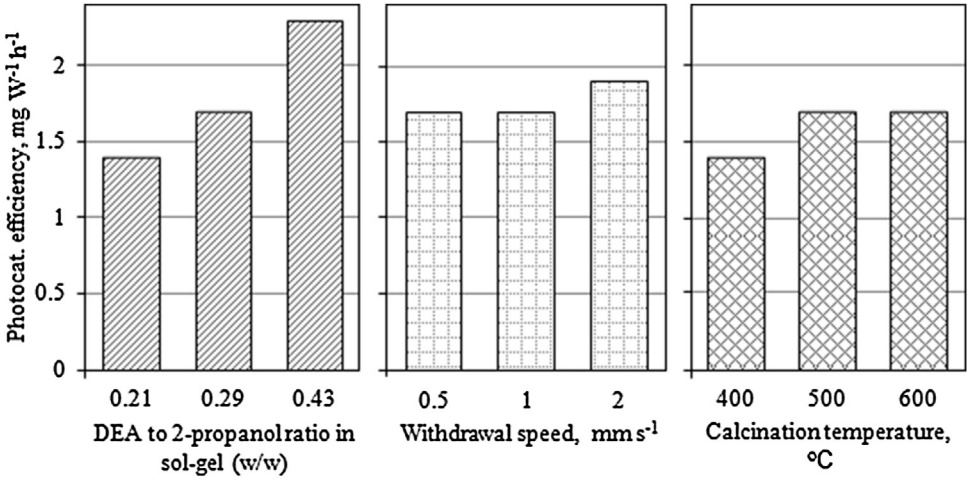

Fig. 4. The impact of DEA to 2-propanol ratio, withdrawal speed and calcination temperature on the photocatalytic activity of sol–gel coatings.

repeated dippings influence the thickness of the coatings and this could be followed in the SEM micrographs.

The increase, for example, in the substrate withdrawal speed from 1 to 2 mm s^{-1} contributing to the coating layer thickening is leading to the sequential development of cracks observed in Fig. 5. The deterioration of coating integrity is reflected in the drop of abrasion resistance characterized by the higher levels of turbidity (Table 1, Series III).

The impact of thermal treatment (Table 1, Series IV and V) showed that mechanical stability of the coatings was not altered by the temperature variations between 400 and 600 °C. The activity of the coated clay, however, was positively influenced by the increase in temperature from 400 to 500 °C (Fig. 4) indicating the possible improvements in titania crystallinity.

The duration of thermal treatment varied from 1 to 3 h, on the opposite, had no effect on the activity of the coatings. However, the prolonged treatment lowered the coated clay's abrasion resistance as the turbidity increased in the course of fluidized operation with every additional hour of calcination (from 23 to 31 FAU) pointing out the changes in coatings microstructure.

The coatings' attrition was also studied varying such fluidized-bed reactor operation parameter as loading of coated clay granules in the reactor: twofold decrease in the amount of coated bed material per volume of treated solution from 17.5 to 8.8 g L^{-1} led to the decrease in turbidity for over 6.5 times (from 27 to 4 FAU), whereas the 35% loss in activity was observed (from 1.7 to 1.1 mg W^{-1} h^{-1}). The optimal bed material loading at the particular UV-A light intensity is currently under study in the larger-scale fluidized-bed reactor.

4. Discussion

4.1. Industrial sols and TBOT-based sol–gel coatings

Low adhesion of the industrial sols on the bed material could be attributed to two factors: the surface of such supporting material as expanded clay is not absolutely inert (towards the coatings solution), because the presence of typical ceramic components, like CaO or Fe_2O_3, influences the acid–base equilibrium (a), and the nanoparticles' sols are very pH-sensitive (b). For example, the XXS 100 sol stability (in terms of nanoparticles agglomeration) was previously found to be pH-dependent [28], whereas expanded clay granules shift the pH of ethanol-diluted XXS solution, for example, from ca. 1.95 to 2.3 (in ca. 40% expanded clay slurry in 2 min contact time); moreover, expanded clay granules shift the pH of water noticeably (e.g. from ca. pH 6.5 to 9 in 8% slurry in 30 min). As a result, the agglomerated TiO_2 nanoparticles could not be firmly fixed on the support material and are washed out. The TTIP-based sol–gel solution with DEA included in its composition allowed to avoid these issues.

4.2. TTIP-based sol–gel coatings

4.2.1. TTIP-based coatings without P25 addition

Zero levels of turbidity of doxycycline solutions treated in a fluidized bed mode, in the case of TTIP-based coatings without P25 addition, indicate that sol *per se* has good adhesion to such material as expanded clay with no cracks formation as was confirmed by the SEM study. The photocatalytic activity of these coatings (Table 1, Series I) is attributed only to the titania formed from TTIP precursor (with no photolysis of doxycycline observed and with the adsorption being previously withdrawn). The temperature of coatings thermal treatment (500 °C) is high enough for the anatase crystallization [29] (see Supplementary materials, Fig. S1, peak of anatase on XRD diagram at $2\theta = 25.3$). The need to enhance the coatings activity was expectedly met by the addition of P25 to the sol–gel solution.

4.2.2. TTIP-based coatings modified by P25

The SEM micrographs of modified sol–gel coatings on expanded clay displayed clearly the change in surface morphology and the appearance of cracks with the increase in P25 particles loading. The addition of P25 to the sol–gel enhancing the coatings activity increases, on the other side, the turbidity of treated solutions with cracks being observed in SEM micrographs at higher P25 contents (5.5 wt%). The improvements in coatings' mechanical properties due to ultrasonication of P25 2-propanol suspension before its addition to the sol–gel solution could be explained by break-up of the largest nanoparticles' agglomerates into the smaller fragments. As a consequence of the more even distribution of P25 powder in sol–gel, less cracking and catalyst washout were achieved. The increase in sol–gel viscosity with the raise of P25 powder content causes also presumably the formation of coatings with increased thickness analogously to the observations in the case of DEA/2-propanol ratio variation in TTIP sol–gel discussed further.

4.2.3. Influence of variations in TTIP-based coatings processing parameters

The variations in sol viscosity, the support withdrawal speed and the number of bed material dippings in the sol–gel are foreseen

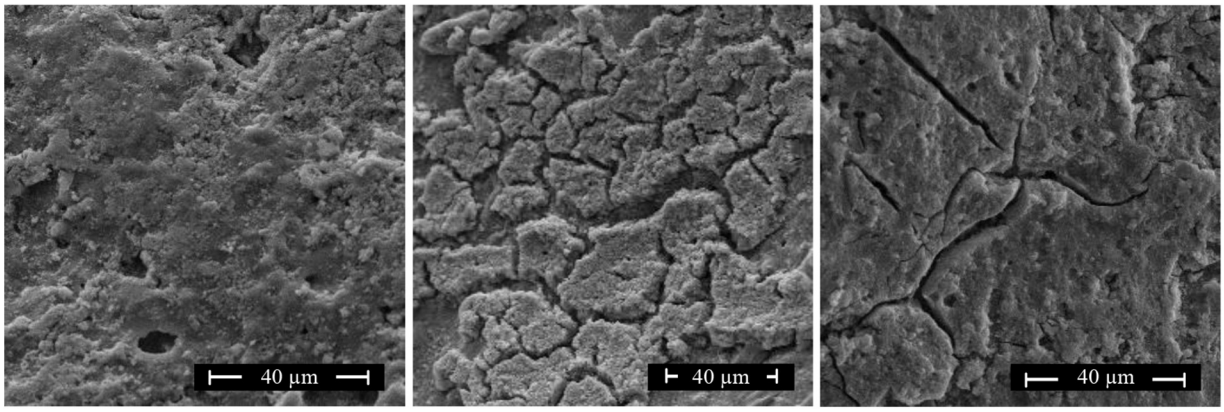

Fig. 5. SEM images of the TTIP-based coatings prepared with substrate withdrawal speed 1 mm s^{-1} (left), 2 mm s^{-1} (middle) and with DEA to 2-propanol ratio of 0.43, w/w (right).

to influence the coatings' properties [30]. However, the texture of substrate material is also determining the quality and properties of coatings resulting in different morphologies and adhesion on various substrates (Shan et al., 2010).

The dilution of P25-modified sol–gel solution, i.e. the decrease in DEA to 2-propanol ratio with P25 content remained constant, caused the reduction in sol–gel viscosity and in the TTIP content inducing the drop in photocatalytic activity of coated clay. While the trend in turbidity changes with a minimum observed with the average DEA to 2-propanol ratio (Table 1, Series II) could be attributed to the variations in the morphology of sol–gel coatings. The SEM study shows the formation and propagation of cracks within the coatings from the sol–gel solution of higher viscosity (Fig. 5), thus favoring the coatings detachment and P25 particles washout. The coatings from the sol–gel solutions of lower viscosity, on the contrary, show the increase in turbidity because of insufficient anchoring of P25 agglomerates with no formation of cracks observed.

The higher withdrawal speed and the repetitive number of dippings of expanded clay in sol–gel result in the increase in the coatings' thickness, thus contributing to the formation of cracks responsible for the enhanced levels of turbidity and deterioration of coated bed material long-term performance in fluidized bed reactor.

The temperature increase from 500 to 600 °C did not altered the activity of coatings, while lower temperature (400 °C) was considered to be not sufficient for the sol–gel thermal treatment with a decrease in activity observed (Fig. 4).

The formation of cracks jeopardizes the long-term efficiency of coated clay, to be used as the bed for fluidization, and the routes to obtain more intact coatings, including intensive deagglomeration of P25 in sol–gel with its subsequent dilution, could be established. Whereas, specific set-up proportions are relevant only for particular material of support, as for stainless steel, for example, Chen and Dionysiou [31] found the optimal concentration of P25 in the sol–gel to be higher than this for expanded clay settled in present study.

The intact coatings with additional titania crystallites evenly distributed within the sol–gel films of optimized thickness meet the requirements for coatings with good mechanical properties and satisfactory photocatalytic antibiotic oxidation efficiency. Search for the optimum between these two characteristics (activity vs. adhesion and attrition) based on the results of doxycycline photocatalytic degradation efficiency and turbidity measurements suggests the following preparation procedure: TTIP/DEA/2-propanol mass ratio of 1:1.5:3.5, P25 content of 2.0 wt%, withdrawal speed of 1 mm s^{-1}, thermal treatment at 500 °C for max 1 h with heating gradient to be optimized. This way

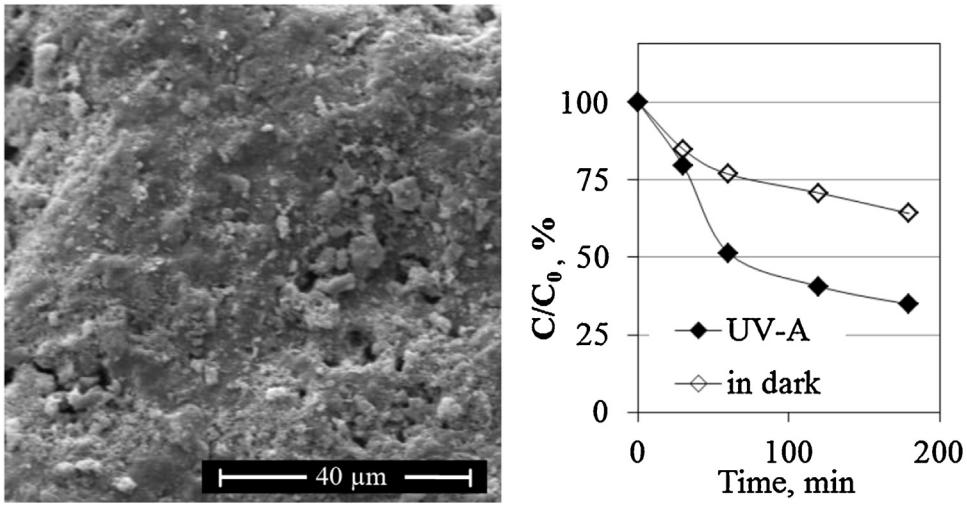

Fig. 6. SEM image and performance of TTIP-based coating prepared using optimized processing parameters.

prepared coatings revealed intact structures characterized also by low turbidity levels (not exceeding 14 FAU) and distinct photocatalytic activity (Fig. 6).

5. Conclusions

The prerequisite for the photocatalytic fluidized-bed reactor development is the elaboration of the coated lightweight materials of satisfactory abrasion resistance and activity as these are subjected to the attrition during the reactor operation.

The implementation of titania sol–gel-coated porous expanded clay granules as support material allows using the benefits of water treatment methods' combination successfully adsorbing pollutants with their subsequent photocatalytic oxidation.

Within the variety of studied sol–gel compositions, based on TTIP and TBOT titania precursors and Hombikat XXS 100 and S5-300A industrial sols, titania coatings on expanded clay prepared using TTIP were found to be the most mechanically stable.

The measurable degradation of doxycycline with zero turbidity in treated solutions is an indicator of photocatalytic activity of intact coatings formed from starting TTIP based sol–gel composition. The increase in the coating thickness deteriorates their quality entailing the formation of cracks and causing the detachment and turbidity raise. The addition of P25 enhances the coatings activity changing also distinctly their morphology as the appearance of cracks with the increase in P25 content is observed, whereas the better P25 particles deagglomeration in the sol–gel is contributing to the coatings properties improvement.

It could be concluded that titania fixation on lightweight expanded clay aggregates by means of sol–gel produced stable and active coatings with properties dependent on the processing parameters. The final choice of fluidized-bed material coatings' preparation parameters is a compromise between coatings' photocatalytic activity, on the one hand, and their adhesion and attrition properties, on the other hand. The interrelation of these characteristics will be further influenced by the operation parameters of fluidized-bed reactor.

Acknowledgements

The financial support from the Estonian Research Council (grant G8978, projects SF0140022s10 and IUT1-7), European Social Fund's Doctoral Studies and Internationalisation Programme DoRa and Archimedes Foundation project 3.2.0801.11-0009 is greatly appreciated. The authors express their gratitude to the Deutsche Forschungsgesellschaft (DFG) (grants DE 598/26-1 and WE 2331/17-1). We thank Tatjana Rudenko for assistance in the laboratory, Juri Pronin for assistance with laboratory apparatus, Thomas Peter and Dr. Mart Viljus for SEM and Adelheid Lüer for BET analyses.

Appendix A. Supplementary data

Supplementary data associated with this article can be found, in the online version, at http://dx.doi.org/10.1016/j.apcatb.2014.10.006.

References

[1] K.D. Brown, J. Kulis, B. Thomson, T.H. Chapman, D.B. Mawhinney, Sci. Total. Environ. 366 (2006) 772–783.
[2] Z. Dong, D.B. Senn, R.E. Moran, J.P. Shine, Regul. Toxicol. Pharm. 65 (2013) 60–67.
[3] K. Ikehata, N.J. Naghashkar, M.G. Ei-Din, Ozone Sci. Eng. 28 (2006) 353–414.
[4] A. Nikolaou, S. Meric, D. Fatta, Anal. Bioanal. Chem. 387 (2007) 1225–1234.
[5] S. Mompelat, B. Le Bot, O. Thomas, Environ. Int. 35 (2009) 803–814.
[6] PAN, Demands for Improved Protection of the Environment from the Adverse Effects of Veterinary Medical Products, Veterinary Pharmaceuticals, PAN Germany, 2013.
[7] D. Klauson, J. Babkina, K. Stepanova, M. Krichevskaya, S. Preis, Catal. Today 151 (2010) 39–45.
[8] D. Klauson, M. Krichevskaya, M. Borissova, S. Preis, Environ. Technol. 31 (2010) 1547–1555.
[9] D. Klauson, A. Poljakova, N. Pronina, M. Krichevskaya, A. Moiseev, T. Dedova, S. Preis, J. Adv. Oxid. Technol. 16 (2013) 234–243.
[10] Y. Zhang, J.C. Crittenden, D.W. Hand, D.L. Perram, Environ. Sci. Technol. 28 (1994) 435–442.
[11] T. Torimoto, S. Ito, S. Kuwabata, H. Yoneyama, Environ. Sci. Technol. 30 (1996) 1275–1281.
[12] H.Y. Ha, M.A. Anderson, J. Environ. Eng.-ASCE 122 (1996) 217–221.
[13] N.J. Peill, M.R. Hoffmann, J. Sol. Energ.-T ASME 119 (1997) 229–236.
[14] S. Preis, M. Krichevskaya, A. Kharchenko, Water Sci. Technol. 35 (1997) 265–272.
[15] P.S. Mukherjee, A.K. Ray, Chem. Eng. Technol. 22 (1999) 253–260.
[16] R.L. Pozzo, J.L. Giombi, M.A. Baltanas, A.E. Cassano, Catal. Today 62 (2000) 175–187.
[17] L. Zhang, Y.F. Zhu, Y. He, W. Li, H.B. Sun, Appl. Catal. B 40 (2003) 287–292.
[18] S. Gelover, P. Mondragon, A. Jimenez, J. Photochem. Photobiol. A 165 (2004) 241–246.
[19] T. Kanki, S. Hamasaki, N. Sano, A. Toyoda, K. Hirano, Chem. Eng. J. 108 (2005) 155–160.
[20] J.M. Kwon, Y.H. Kim, B.K. Song, S.H. Yeom, B.S. Kim, J.B. Im, J. Hazard. Mater. 134 (2006) 230–236.
[21] A.Y. Shan, T.I.M. Ghazi, S.A. Rashid, Appl. Catal. A 389 (2010) 1–8.
[22] J.W. Shi, H.J. Cui, J.W. Chen, M.L. Fu, B. Xu, H.Y. Luo, Z.L. Ye, J. Colloid. Interf. Sci. 388 (2012) 201–208.
[23] D.S. Selishchev, P.A. Kolinko, D.V. Kozlov, J. Photochem. Photobiol. A 229 (2012) 11–19.
[24] M. Zendehzaban, S. Sharifnia, S.N. Hosseini, Kor. J. Chem. Eng. 30 (2013) 574–579.
[25] X.X.S. Hombikat, 100, Product Information, Sachtleben Chemie GmbH, 2006.
[26] CristalACTiV S5-300A, Product Data Sheet, Cristal (2012).
[27] S. Preis, M. Krichevskaya, Y. Terentyeva, A. Moiseev, J. Kallas, J. Adv. Oxid. Technol. 5 (2002) 77–84.
[28] A. Matthias, Lichtwellenleitung in TiO_2-Schichten aus dispergierten Nanopartikeln auf Glas, PhD Thesis, TU Clausthal, 2014.
[29] S.H. Oh, J.S. Kim, J.S. Chung, E.J. Kim, S.H. Hahn, Chem. Eng. Commun. 192 (2005) 327–335.
[30] C.J. Brinker, A.J. Hurd, P.R. Schunk, G.C. Frye, C.S. Ashley, J. Non-Cryst. Solids 147–148 (1992) 424–436.
[31] Y.J. Chen, D.D. Dionysiou, Appl. Catal. B 62 (2006) 255–264.